Salmonella Typhimurium utilizes a T6SS-mediated antibacterial weapon to establish in the host gut

Thibault G. Sana[a], Nicolas Flaugnatti[b], Kyler A. Lugo[a], Lilian H. Lam[a], Amanda Jacobson[a], Virginie Baylot[c], Eric Durand[b], Laure Journet[b], Eric Cascales[b], and Denise M. Monack[a,1]

[a]Department of Microbiology and Immunology, Stanford School of Medicine, Stanford University, Stanford, CA 94305; [b]Laboratoire d'Ingénierie des Systèmes Macromoléculaires (UMR7255), Institut de Microbiologie de la Méditerranée, Aix-Marseille Université - CNRS, 13402 Marseille, France; and [c]Division of Oncology, Department of Medicine and Pathology, Stanford School of Medicine, Stanford University, Stanford, CA 94305

Edited by Scott J. Hultgren, Washington University School of Medicine, St. Louis, MO, and approved June 30, 2016 (received for review June 2, 2016)

The mammalian gastrointestinal tract is colonized by a high-density polymicrobial community where bacteria compete for niches and resources. One key competition strategy includes cell contact-dependent mechanisms of interbacterial antagonism, such as the type VI secretion system (T6SS), a multiprotein needle-like apparatus that injects effector proteins into prokaryotic and/or eukaryotic target cells. However, the contribution of T6SS antibacterial activity during pathogen invasion of the gut has not been demonstrated. We report that successful establishment in the gut by the enteropathogenic bacterium *Salmonella enterica* serovar Typhimurium requires a T6SS encoded within *Salmonella* pathogenicity island-6 (SPI-6). In an in vitro setting, we demonstrate that bile salts increase SPI-6 antibacterial activity and that *S.* Typhimurium kills commensal bacteria in a T6SS-dependent manner. Furthermore, we provide evidence that one of the two T6SS nanotube subunits, Hcp1, is required for killing *Klebsiella oxytoca* in vitro and that this activity is mediated by the specific interaction of Hcp1 with the antibacterial amidase Tae4. Finally, we show that *K. oxytoca* is killed in the host gut in an Hcp1-dependent manner and that the T6SS antibacterial activity is essential for *Salmonella* to establish infection within the host gut. Our findings provide an example of pathogen T6SS-dependent killing of commensal bacteria as a mechanism to successfully colonize the host gut.

antiprokaryotic activity | T6SS SPI-6 | *Salmonella* Typhimurium | gut microbiota | colonization

Infections by enteric microbial pathogens begin upon invasion of the intestinal tract, where survival and replication are necessary for transmission to occur. This environment, however, is already colonized by a high-density population of commensals and other microorganisms that directly interact with the pathogen and modulate its colonization. Previous work has shown that the microbiota provides colonization resistance against pathogens through a myriad of roles involving host tissue development, physiology, and mucosal immunology (1, 2). This phenomenon is mediated by secretion of antimicrobial peptides, competition for nutrients, and immune modulation by specific phylogenetic groups (3–6). In addition, bacteria often exhibit direct antagonistic behavior toward each other in microbial communities by delivering antibacterial toxins into competitors (7).

To survive in a multispecies environment such as the gastrointestinal tract, bacterial pathogens have developed various strategies to compete with other species and acquire access to nutritional and spatial niches. For example, some bacteria exert long-range inhibitory effects by secreting diffusible molecules such as antibiotics, bacteriocins, and H_2O_2 (8). Interestingly, previous studies have shown that one molecular mechanism mediating such behavior is the widely conserved type VI secretion system (T6SS) (9). Many sequenced genomes of Gram-negative bacteria encode a T6SS, which could be present in more than one copy (10, 11). The T6SS is widespread in Gram-negative bacteria, with an overrepresentation in γ-*Proteobacteria*, particularly in *Enterobacteriaceae* (11, 12). T6SSs are versatile systems that deliver toxins into either eukaryotic or prokaryotic cells, or both (10). For example, the *Vibrio cholerae* Vas and the *Pseudomonas aeruginosa* H2-T6SS target and kill bacteria but also inject toxins into host cells to prevent phagocytosis or to facilitate invasion, respectively (13–18). The T6SS is a multiprotein machine that uses a contractile mechanism for toxin secretion (19). In short, the T6SS comprises a transenvelope complex that docks a contractile tail composed of an inner tube, made of stacked Hcp protein hexamers, tipped by the VgrG syringe, and surrounded by a sheath, comprising polymerized TssB and TssC subunits (20–22). Sheath contraction provides the energy necessary for the injection of the toxins that are confined within the Hcp tube or bound to VgrG (23). After injection, the ClpV ATPase recycles the contracted sheath to permit a new assembly/injection step to occur (24).

Salmonella enterica serovar Typhimurium is a leading cause of human gastroenteritis worldwide and causes a typhoid-like disease in mice. Because this pathogen is transmitted by the fecal–oral route, it spends a significant part of its life cycle within intestinal microbial communities. Although absence of the microbiota allows the pathogen to multiply to high densities (25), a high-complexity microbiota facilitates *S.* Typhimurium clearance (26). This not only illustrates the critical role of the intestinal microbiota in modulating *Salmonella* infection, but also suggests that *Salmonella* must modulate its interactions with the microbiota (27). Several reports have shown that acute inflammation triggered by *S.* Typhimurium modifies the gut bacterial community to facilitate pathogen colonization in a mouse model (28–32). However, it is currently unknown whether *Salmonella* can directly target commensal bacteria with an antibacterial activity.

Significance

Gram-negative bacteria use the type VI secretion system (T6SS) to deliver effectors into adjacent cells. *Salmonella* Typhimurium is an enteric pathogen that causes disease in millions of individuals each year. Its ability to infect the mammalian gut is a key factor that contributes to its virulence and transmission to new hosts. However, many of the details on how *Salmonella* successfully colonizes the gut and persists among members of the gut microbiota remain to be deciphered. In this work, we provide evidence that *Salmonella* uses an antibacterial weapon, the type VI secretion system, to establish infection in the gut. In addition, our results suggest that *S.* Typhimurium selectively targets specific members of the microbiota to invade the gastrointestinal tract.

Author contributions: T.G.S., E.C., and D.M.M. designed research; T.G.S., N.F., K.A.L., L.H.L., A.J., V.B., and E.D. performed research; T.G.S., N.F., K.A.L., E.D., L.J., E.C., and D.M.M. analyzed data; and T.G.S., E.C., and D.M.M. wrote the paper.

The authors declare no conflict of interest.

This article is a PNAS Direct Submission.

Freely available online through the PNAS open access option.

[1]To whom correspondence should be addressed. Email: dmonack@stanford.edu.

This article contains supporting information online at www.pnas.org/lookup/suppl/doi:10.1073/pnas.1608858113/-/DCSupplemental.

The genome of *S.* Typhimurium encodes a T6SS within the *Salmonella* pathogenicity island 6 (SPI-6) locus that is well conserved among *S. enterica* serovars (33). In addition to the structural components of the T6SS, the SPI-6 locus encodes two Hcp subunits, Hcp1 and Hcp2 (33), as well as Tae4, an antibacterial amidase with homologs in other bacteria (34) (Fig. S1). Tae4 induces bacterial lysis by cleaving the γ-D-glutamyl-L-*meso*-diaminopimelic acid amide bond of peptidoglycan and is toxic when expressed in a laboratory strain of *Escherichia coli* (34, 35). Furthering this idea, it has recently been reported that the SPI-6 T6SS is required for *S.* Typhimurium to outcompete a laboratory strain of *E. coli* in vitro (36). However, the contribution of the T6SS antiprokaryotic activity of *S.* Typhimurium during infection of the gut remains unknown.

In this work, we show that a SPI-6–deficient *S.* Typhimurium mutant is impaired in intestinal colonization. We show that SPI-6–mediated killing is magnified by the presence of bile salts and is required for killing members of the gut microbiota in vitro, such as *Klebsiella oxytoca.* We observe that the SPI-6–mediated antibacterial activity against *K. oxytoca* requires the Hcp1 protein but is independent of Hcp2. We report that only Hcp1 binds to the Tae4 antibacterial toxin, suggesting that Hcp proteins select the effectors to be secreted. Additionally, we demonstrate that the antibacterial activity of SPI-6 against *K. oxytoca* occurs in vivo in the mouse gut, and we provide evidence that Hcp1-mediated antibacterial activity is necessary for *Salmonella* establishment within the gut.

Results

S. Typhimurium SPI-6 Is Required for Colonization in the Mouse Gut. Although the type VI secretion system has been proposed to shape bacterial communities in vitro, little is known about its role in vivo. To test whether the *S.* Typhimurium SPI-6–encoded T6SS plays a role in the colonization of the gastrointestinal tract, we orally infected 129x1/SvJ mice with either WT *S.* Typhimurium or an isogenic mutant lacking the entire SPI-6 locus, represented in Fig. S1 (Δ*SPI-6*). We have previously shown that the level of *S.* Typhimurium excreted in the feces is identical to the levels in the cecum and colon during the first 35 d postinfection (37). Thus, we quantitated the levels of WT and mutant bacteria excreted in the feces of individual mice over time. The levels of WT *S.* Typhimurium were significantly higher than the Δ*SPI-6* mutant at 5 d postinfection (Fig. 1*A*). In addition, we noted a striking difference in the ability of these strains to expand in the gut. Although the levels of WT bacteria increased 100-fold during the first 18 d of infection, the Δ*SPI-6* mutant did not significantly expand (Fig. 1*A*). We next tested the role of SPI-6 in *S.* Typhimurium colonization of systemic tissues after oral infection. The levels of WT and SPI-6–deficient bacteria were similar in Peyer's patches (PPs), mesenteric lymph nodes (MLNs), spleen, and liver at 7 d postinfection (Fig. 1*B*). Collectively, our results demonstrate that SPI-6 plays an important role in the colonization of the gut but not in systemic tissues, which raises the question of whether the T6SS encoded on SPI-6 is able to target commensal bacteria within the gut in order for *S.* Typhimurium to successfully establish itself in this niche.

S. Typhimurium T6SS Kills Microbiota Members and Is Enhanced by Bile Salts in Vitro. Previous studies have highlighted that T6SS gene clusters are tightly regulated (38–40). The *S.* Typhimurium SPI-6 T6SS gene cluster is repressed by the DNA-binding protein H-NS and thus limits its antibacterial activity (36). However, H-NS is a global regulator that controls the expression of multiple secretion systems and iron acquisition systems. In addition, *S.* Typhimurium H-NS–deficient bacteria grow very slowly compared with WT bacteria and accumulate compensatory mutations over time. Thus, the pleiotropic effects that are associated with H-NS–deficient strains prohibit the use of the *hns* mutant for in vivo and ex vivo experiments, which prompted us to identify signal molecules that activate *S.* Typhimurium T6SS encoded on SPI-6. A previous study demonstrated that the T6SS from *V. cholerae*, an intestinal pathogen, is activated by bile salts (41). Because we found that SPI-6 is important for *S.* Typhimurium to colonize the guts of mice, we tested whether bile salts increase the activity of *S.* Typhimurium SPI-6 T6SS. To test this question, we mixed either WT or Δ*clpV* (ATPase essential for T6SS function) bacterial strains with *E. coli* K-12 on plates containing bile salts. The presence of bile salts increases the ability of *S.* Typhimurium to outcompete *E. coli* K-12 in vitro in a T6SS-dependent manner (Fig. 2*A*).

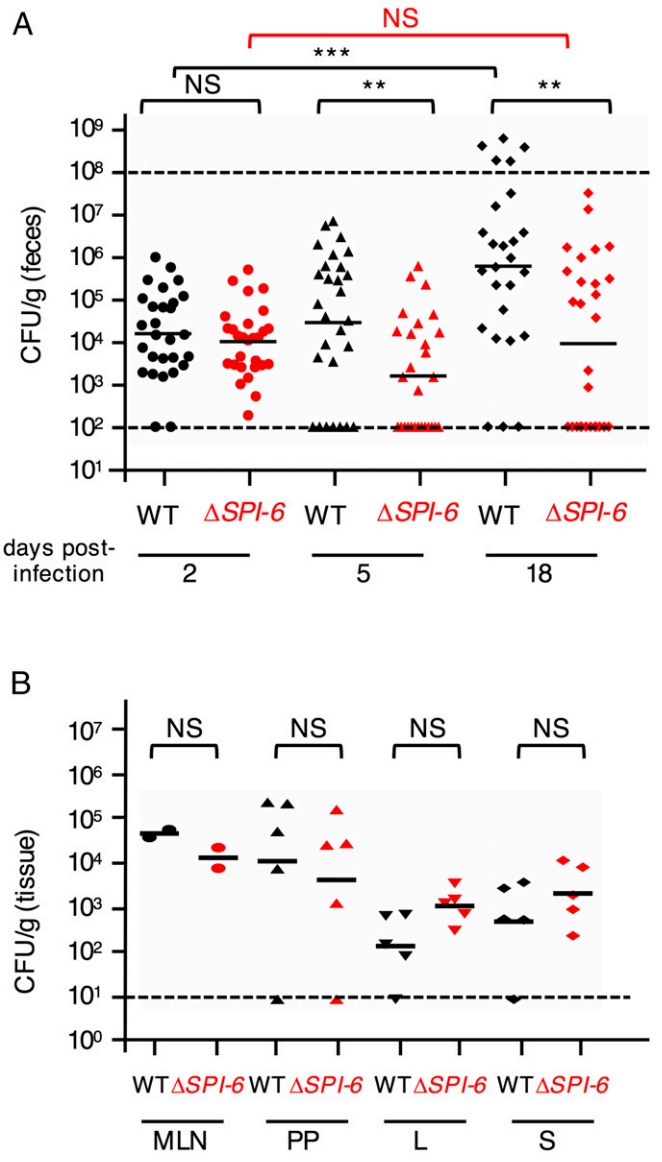

Fig. 1. SPI-6 is important for colonization of the gut. (*A*) The 129x1/SvJ Mice were infected orally with 10^8 WT or Δ*SPI-6* mutant *S.* Typhimurium bacterial strains. Feces were collected and plated over time on media that were selective for *Salmonella*. Every data point represents one mouse, and the bar represents the geometric mean. (*B*) The 129x1/SvJ mice were orally infected with 10^8 WT or Δ*SPI-6 Salmonella* Typhimurium bacterial strains, and tissues were harvested at day 7 postinfection and plated on selective media. Data for mesenteric lymph nodes (MLNs), Peyer's patches (PPs), liver (L), and spleen (S) are shown. Statistical significance is shown based on Mann–Whitney *U* test (NS, not significant; $^{**}P < 0.01$; $^{***}P < 0.001$).

In the mammalian gut, *S.* Typhimurium shares this niche with commensal bacteria from diverse genera, including *Proteobacteria* and *Bacteroidetes*. We first tested the ability of WT or SPI-6–deficient strains to kill representative commensals of the gut microbiota in vitro. Using the conditions described above, we show that *S.* Typhimurium kills *K. oxytoca* and *Klebsiella variicola* in a SPI-6–dependent manner, but not *Enterobacter cloacae* or the *E. coli* JB2 mouse commensal strain (28) (Fig. 2*B*). Finally, *S.* Typhimurium did not outcompete gut commensals such as *Bacteroides fragilis*, *Bifidobacterium longum*, *Parabacteroides distasonis*, and *Prevotella copri* when grown anaerobically on blood plates, a condition in which the SPI-6 T6SS is active, as shown by *S.* Typhimurium's killing of *K. oxytoca* (Fig. S2).

Hcp1, but Not Hcp2, Binds Tae4 and Is Required for Interbacterial Antagonism. T6SS effectors are delivered into target cells by a cargo mechanism using the Hcp hexamer or the VgrG/PAAR spike as a carrier (10, 23, 42–45). The SPI-6 T6SS encodes two distinct Hcp proteins, STM0276 and STM0279, hereafter called Hcp1 and Hcp2, respectively. To test the contribution of these two distinct Hcp proteins for the antibacterial activity, we engineered Δ*hcp1* and Δ*hcp2* mutant strains and performed in vitro competition assays against *K. oxytoca* (Fig. 3*A*). In addition, we constructed a strain deficient for the Tae4 muramidase, Δ*tae4*. The Δ*clpV*, Δ*hcp1*, and Δ*tae4* mutant bacterial strains were attenuated in their ability to kill *K. oxytoca*. In contrast, the Δ*hcp2* mutant outcompeted *K. oxytoca* at levels comparable with the WT *S.* Typhimurium strain (Fig. 3*A*). The ability of the Δ*hcp1* and Δ*tae4* mutant strains to kill *K. oxytoca* was rescued by providing plasmid-borne WT copies of *hcp1* and *tae4* under an arabinose-inducible promoter, respectively (Fig. S3). Taken together, our data indicate that the Hcp1 and Tae4 proteins are specifically required for antibacterial antagonism against commensal *K. oxytoca*.

Silverman et al. previously reported that a subset of T6SS effector proteins, including *P. aeruginosa* Tse1, Tse2, and Tse3, bind the luminal side of the Hcp hexamer. This interaction between Hcp and the effector stabilizes the effector and allows for proper delivery upon sheath contraction (23). To test the interaction of Tae4 with the Hcp1 and Hcp2 proteins, we performed a bacterial two-hybrid assay. Our data indicate that Tae4 binds to Hcp1 but does not interact with Hcp2 (Fig. 3*B*). In addition, the Tae4 and 6×His-tagged Hcp1 and Hcp2 proteins were purified to homogeneity, and interactions were assessed by copurification experiments. The biotinylated Tae4 protein copurified with 6×His-tagged Hcp1 using immobilized metal affinity chromatography but did not precipitate with 6×His-Hcp2 (Fig. 3*C*). Collectively, these results show that the Tae4 effector binds specifically to Hcp1 and suggest that Hcp1 delivers this amidase effector into target cells, which is consistent with the role of Hcp1 in interbacterial antagonism.

The T6SS Antibacterial Activity of *S.* Typhimurium Is Required for Early Establishment Within the Host Gut. Based on our in vitro findings, we hypothesized that *S.* Typhimurium outcompetes *K. oxytoca* within the host gut in a T6SS-dependent manner. To test this notion, we used a mouse model to measure T6SS contact-dependent activity (9). However, *K. oxytoca* does not represent a large portion of the gut microbiota (Fig. S4*A*). Thus, we increased *K. oxytoca* levels in the guts of 129x1/SvJ mice by first treating the mice with a mixture of antibiotics for 2 wk to reduce the number of indigenous commensal bacteria (Fig. S4*A*), followed by oral inoculation of mice with 10^8 *K. oxytoca*. After confirming *K. oxytoca* colonization by plating feces on MacConkey agar (Fig. S4*A*), we orally infected mice with 10^8 WT or Δ*hcp1* *S.* Typhimurium. *K. oxytoca* and *S.* Typhimurium levels were enumerated in the cecum and colon of coinfected mice 3 d postinfection. There was a dramatic decrease in the levels of *K. oxytoca* in the cecum (Fig. 4*A*) and the colon (Fig. S4*B*) of mice coinfected with WT *S.* Typhimurium. In contrast, the levels of *K. oxytoca* remained similar to the input when the mice were coinfected with the Δ*hcp1* mutant bacteria. There were no significant differences in the levels of WT versus Δ*hcp1* *S.* Typhimurium in the guts of the antibiotic-treated mice (Fig. 4*A*). We therefore conclude that the antibacterial activity of SPI-6 is active against *K. oxytoca* in the host gut.

To test whether Hcp1-mediated antibacterial activity mediates establishment of *Salmonella* within unperturbed guts, we orally infected 129x1/SvJ mice with WT, Δ*hcp1,* or Δ*hcp2* bacterial strains and measured cfus in feces over time. Although the levels of WT and T6SS mutant strains were similar for the first 2 d of infection, there were significantly lower levels of the Δ*hcp1* mutant bacterial strain compared with the WT strain 5 d postinfection (Fig. 4*B*). In contrast, the levels of the Δ*hcp2* mutant strain were not significantly different from WT levels (Fig. 4*B*).

Because the intestinal microbiota compositions in 129x1/SvJ and C57BL/6 mice are different (46), we wondered whether the

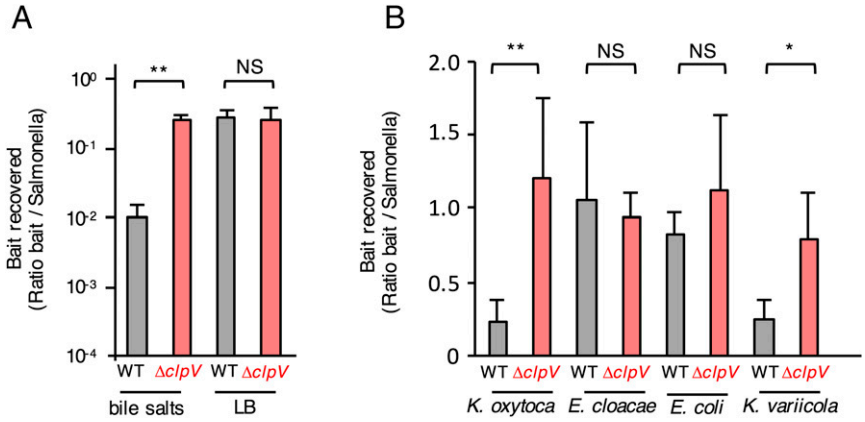

Fig. 2. SPI-6 is activity is enhanced by bile salts and provides competitive advantage against members of the microbiota in vitro. (*A*) WT and mutant *S.* Typhimurium strains were incubated with *E. coli* K-12 DH5α to assess T6SS-dependent killing. The indicated *S.* Typhimurium attacker strain was mixed with *E. coli* prey at a 1:1 ratio and incubated for 48 h on an LB agar plate supplemented or not with 0.05% porcine bile salts. Recovered mixtures were plated onto selective media. (*B*) WT and mutant *S.* Typhimurium strains were incubated with the indicated commensal strains (*K. oxytoca*, *E. cloacae*, *K. variicola*, and *E. coli* JB2) for 48 h on an LB agar plate supplemented with 0.05% porcine bile salts. Recovered mixtures were plated onto selective media. Statistical significance is shown based a Student's *t* test corresponding to the values of the WT strain (NS, not significant; $*P < 0.05$; $**P < 0.01$).

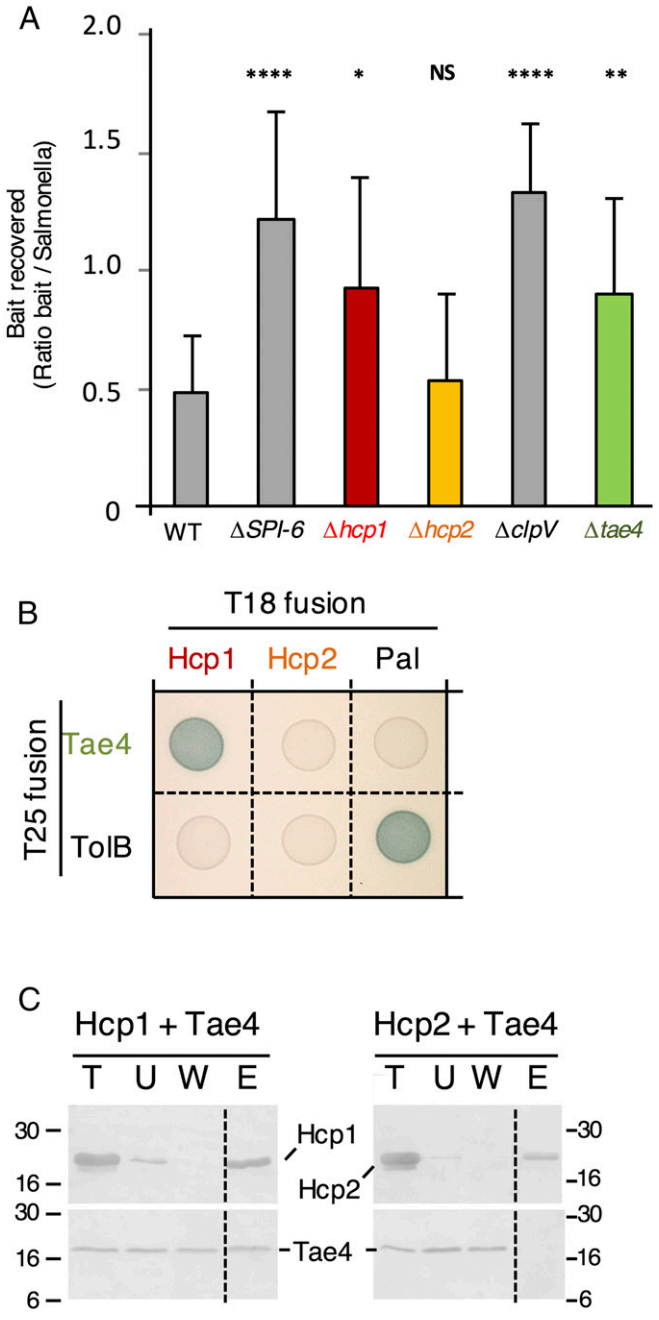

Fig. 3. Hcp1 binds the Tae4 amidase effector and mediates *K. oxytoca* killing. (*A*) WT and mutant *S.* Typhimurium strains were incubated with *K. oxytoca* for 48 h on an LB agar plate supplemented with 0.05% porcine bile salts. Recovered mixtures were plated onto selective media. Statistical significance is shown based on a Student's *t* test corresponding to the values of the WT strain (NS, not significant; $*P < 0.05$; $**P < 0.01$; $****P < 0.0001$). (*B*) Bacterial two-hybrid analyses. BTH101 reporter cells producing the Hcp1 or Hcp2 proteins fused to the T18 domain of the *Bordetella* adenylate cyclase and the Tae4 protein fused to the T25 domain were spotted on plates supplemented with IPTG and the chromogenic substrate X-Gal. Interaction between the two fusion proteins is attested by the blue color of the colony. The TolB-Pal interaction serves as a positive control. (*C*) Coprecipitation assay. Purified and biotinylated Tae4 was mixed with 6×His-tagged Hcp1 (*Left*) or Hcp2 (*Right*) and subjected to ion metal affinity chromatography on Ni^{2+} resin. The total (T), unbound (U), wash (W), and eluted (E) fractions were collected and subjected to SDS/PAGE and Western blot analyses using anti-His antibody (*Upper*) and streptavidin-conjugated alkaline phosphatase (*Lower*). The position of the proteins and the molecular mass markers (in kDa) are indicated.

SPI-6 T6SS is important for *S.* Typhimurium colonization in the gut of C57BL/6 mice. Because *S.* Typhimurium infection of C57BL/6 mice induces high levels of inflammation in the gut at the early time points that we were interested in, we performed a competition assay in which mice were infected with an equal mixture of *S.* Typhimurium WT strain and either an *hcp1* or *hcp2* mutant strain. Feces were collected 1 d and 2 d postinfection, and cecum and colons were harvested on day 3. WT and mutant bacteria were enumerated in each sample by plating on regular and kanamycin-containing plates (to select for the mutant strain). One day postinfection, levels of both WT and mutant bacterial strains were similar in the feces (Fig. 4*C*). Two days postinfection, 10-fold lower levels of the Δ*hcp1* mutant bacteria were recovered compared with WT bacteria (Fig. 4*C*). Similarly, at 3 d postinfection, Δ*hcp1* mutant bacteria were outcompeted in the cecum and colon (Fig. 4*A* and Fig. S4*B*). In contrast, Δ*hcp2* mutant bacteria were present at levels comparable to the WT strain in the feces, cecum, and colon (Fig. 4*C*). Collectively, these results suggest that Hcp1-dependent antibacterial activity is essential for successful colonization of the gut.

From these results, we conclude that the Hcp1-mediated antibacterial activity of the SPI-6 T6SS confers a competitive advantage to *S.* Typhimurium against the gut microbiota and facilitates *S.* Typhimurium establishment in multispecies communities. Because these results could be due to different bacterial burdens between our mutants, we decided to treat mice orally with a mixture of antibiotics for 2 wk, which has been previously shown to reduce the inherent colonization resistance against *S.* Typhimurium mediated by the indigenous microbiota (47). After antibiotic treatment, we orally gavaged equivalent numbers of WT, Δ*hcp1*, Δ*hcp2*, or Δ*tae4* mutant bacteria. WT and mutant bacteria colonized the guts of the antibiotic-treated mice at high, comparable levels (Fig. S5). These results indicate that, in the absence of an intact commensal microbial community, the antibacterial weapon of *S.* Typhimurium is not required to establish in the gut.

Discussion

In nature or within hosts, microbes often exist in complex communities, and therefore they must compete with other species for limited resources. Many Gram-negative bacteria encode a molecular machine called the T6SS that is dedicated to target and kill other bacteria and sometimes to inject effector proteins into eukaryotic cells (10). For example, the human pathogen *V. cholerae* employs the T6SS to kill *E. coli* or to disable the amoebae *Dictyostelium discoideum* and macrophage cell lines (14, 48, 49). Recent studies demonstrated that T6SS organelles in *V. cholerae*, *P. aeruginosa*, and entero-aggregative *E. coli* cells are very dynamic and likely expel their T6SS spike/tube VgrG/Hcp complex toward prokaryotic cells and cause target cell lysis by delivering antibacterial toxins (50, 51). A broad diversity of antibacterial toxins have been described so far (10, 42). In this work, we show that the SPI-6 T6SS is required for efficient *Salmonella* establishment in the gut and that it is the antibacterial activity of the T6SS that contributes to this phenotype, suggesting a direct interaction between the pathogen and the indigenous microbiota. In vitro competition assays demonstrated a SPI-6 T6SS-dependent killing of members of the gut microbiota in vitro, which was confirmed by in vivo survival assays. Finally, we provide details on the molecular mechanism underlying SPI-6–mediated competition by showing that the Tae4 amidase interacts with Hcp1, facilitating its delivery and activity within prey bacterial cells. This report demonstrates that the antibacterial activity of a T6SS is important for a pathogen to establish within the host gut and opens new exciting perspectives.

In addition to the core set of 13 genes required for T6SS assembly and function, the *S.* Typhimurium SPI-6 locus contains two copies of the *hcp* gene, *hcp1* and *hcp2* (33). Hcp proteins

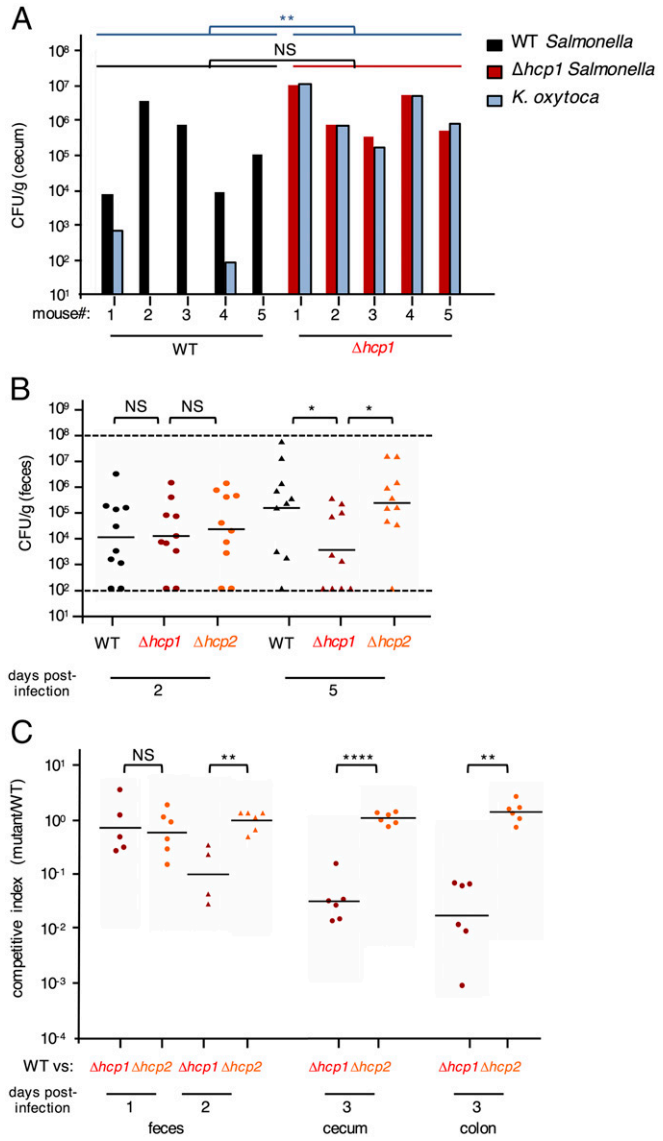

Fig. 4. *S.* Typhimurium SPI-6 antibacterial activity is active in vivo and mediates pathogen establishment in the host gut. (*A*) The 129x1/SvJ mice were treated with antibiotics for 2 wk before colonization with *K. oxytoca*. The day after, mice were infected orally with either 10^8 WT or Δ*hcp1* mutant *S.* Typhimurium bacterial strain. The cecum was harvested from each mouse, homogenized, and plated at day 3 postinfection. The levels of *S.* Typhimurium and *K. oxytoca* were determined and represented as paired bars for each mouse. (*B*) The 129x1/SvJ Mice were infected orally with either 10^8 WT or Δ*hcp1* mutant *S.* Typhimurium bacterial strain. Feces were collected and plated over time on *Salmonella* selective medium. Every data point represents one mouse, and the bar represents the geometric mean. Statistical significance is shown based on Mann–Whitney *U* test (NS, not significant; $*P < 0.05$). (*C*) C57BL/6 mice were infected orally with a 1:1 mixture of WT bacteria and the indicated bacterial mutant strain (5×10^8 cells of each *S.* Typhimurium strain). Feces were collected at day 1 or 2 whereas cecum and colon tissues were harvested at day 3 postinfection and plated on *Salmonella* selective medium. The data represent the competitive index (CI) value for the cfu mutant/WT bacteria in the feces at days 1 or 2. Bars represent the geometric mean CI value for each group of mice. Statistical significance is shown based on the ANOVA with a Dunnett's posttest compared with the corresponding CI values of the Δ*hcp2* mutant (NS, not significant; $**P < 0.01$; $****P < 0.0001$).

assemble hexamers that stack on each other to form the T6SS tail tube (52, 53). In addition to being a structural component of the apparatus, Hcp hexamers are delivered into target cells and serve as chaperone and cargo for toxin effectors (23, 53). The *S.* Typhimurium Hcp1 and Hcp2 proteins share 94% identity and differ by only 10 residues (Fig. S6*A*). However, *S.* Typhimurium has evolved to specifically use the Hcp1 protein to target bacterial cells because *hcp1*—but not *hcp2*—is required for bacterial killing. This specificity is conferred by the ability of Hcp1 to specifically bind the antibacterial Tae4 toxin (Fig. 3 *B* and *C*). Based on electron micrographs, Silverman et al. recently proposed that effectors bind inside the lumen of the Hcp tube (23). Intriguingly, molecular modeling of the Hcp1 and Hcp2 hexamers demonstrate that 4 out of the variable 10 residues, including residues 124 and 125, are predicted to face the lumen (Fig. S6*B*). These differences might explain the specificity of interaction with different effectors. Interestingly, Zhou et al. previously reported that Hcp1 and Hcp2 of *E. coli* K1 have differential roles in binding and invading human endothelial cells and in actin cytoskeleton rearrangement, respectively, suggesting a similar mechanism of binding to different effectors (54). Therefore, this mechanism of specificity could be common among T6SSs. It is also important to note that two variable residues, at position 115 and 116, located at the hexamer–hexamer interface. These differences might mediate specificity between Hcp interactions and prevent assembly of Hcp1/Hcp2 hetero-tubes.

Previous studies on the mechanisms of *S.* Typhimurium colonization of the mouse gut have shown that *Salmonella* exploits intestinal inflammation to compete with the resident microbiota and to thrive in the inflamed gut (28–32). All these previous studies have been performed in mice that have been pretreated with an antibiotic (e.g., streptomycin) that perturbs the indigenous microbiota. We have shown that, in the absence of antibiotic pretreatment, *S.* Typhimurium uses its T6SS to colonize the gut within the first 2–5 d of infection. Furthermore, we observed the contribution of the antibacterial-specific factors at times in which we do not detect signs of inflammation based on histopathology, fecal cytokine levels, and flow cytometry (55). Our results strongly suggest that an active Hcp1-dependent delivery of Tae4 directly targets the resident microbiota, leading to an efficient establishment in the host gut. Surprisingly, this phenotype is seen in both 129x1/SvJ and C57BL/6 mice although their respective commensal microbiota is profoundly different (46), suggesting a mechanism that has evolved to face a wide variety of bacteria to establish within the gut. Finally, the antibacterial action of the *S.* Typhimurium SPI-6 T6SS within the gut is supported by the observation that killing of prey bacteria is enhanced in the presence of bile salts (Fig. 2*A*), a result similar to that observed for mucin activation and bile salts activation of the *V. cholerae* T6SS within the mouse gut (41).

One can ask whether SPI-6 specifically delivers effectors to selected commensal bacteria. Among the strains tested, we identified two commensals that are killed in a SPI-6–dependent manner, *K. oxytoca* and *K. variicola*. In a recent report, it has been suggested that *K. oxytoca* and *S.* Typhimurium metabolize the same oxidized sugars within the gut (56). In this scenario, it would be advantageous for the pathogen to kill direct competitors for the same food. However, this mechanism of direct killing of competitors is only effective for some species that are sensitive to *Salmonella*'s T6SS. For example, we found that *E. cloacae* is not killed by the SPI-6 attack. This result is in agreement with the fact that the genome of *E. cloacae* encodes a Tai4 immunity protein that has been shown to bind and inhibit *S.* Typhimurium Tae4 activity (35, 57). In our study, we found that the ability of *S.* Typhimurium to kill *E. coli* was strain-dependent. We were surprised that, in contrast to the *E. coli* K-12 DH5α or W3110 laboratory strains (this study and ref. 36), the commensal *E. coli* JB2 strain was resistant to SPI-6 attack, which suggests that a defense mechanism may be present in the commensal strain, such as the presence of a T6SS gene cluster or cross-immunity via a Tai4 homolog. Alternatively, it was shown that resident commensal *E. coli* and *S.* Typhimurium may transiently cooperate

in the gut during inflammation (31), suggesting that perhaps a secondary mechanism is at play. Although we have shown that *K. oxytoca* is one target of the *S.* Typhimurium T6SS in vivo, future studies will be necessary to determine whether other members of the gut microbiota are also targeted via this secretion machinery in vivo.

Intriguingly, other gut pathogens such as *Campylobacter jejuni*, *Helicobacter hepaticus*, and *V. cholerae* also have a T6SS, and it would be interesting to determine whether gut colonization by these pathogens is mediated through a potential antibacterial activity (58–60). Altogether, this new colonization strategy could be a common theme among Gram-negative gut pathogens, and T6SS-mediated antibacterial interactions should be further studied to have a more comprehensive understanding of the interaction between the pathogen and the host in its entirety. The role of T6SS in host colonization is a new and exciting area of exploration. Recently, it has been shown that some members of the microbiota have a T6SS that is active against other bacteria (61). Moreover, it was reported that about half of the *Bacteroidales* genomes, the most prevalent Gram-negative bacterial order of the human gut, encode at least one T6SS (62). Finally, a recent report shows that the T6SS is important for *B. fragilis* to outcompete other commensal bacteria in vitro and that this T6SS is active in vivo, suggesting a role in the gut colonization for this commensal (63).

In our work, we provide evidence of an enteric pathogen using a T6SS against the microbiota, leading to establishment in the host gut. Therefore, this work provides strong evidence for considering a new important player for the battle in the gut that is directed by the T6SS, which facilitates a fine-tuned killing mechanism that selectively eliminates competing members of the microbiota (e.g., *K. oxytoca*) but leaves cross-feeding bacterial members alive. In addition, members of the microbiota that possess a functional T6SS may implement a counterattack in this war against the pathogen. We could then imagine a T6SS-directed war in the gut between commensal microbiota and pathogenic bacteria. It is interesting to note that the *hcp1* mutant is not rescued by WT *S.* Typhimurium in the coinfection model (Fig. 4*C*). Even if the WT and mutant bacteria were occupying the same spatial niche, the *hcp1* mutant would still be at a competitive disadvantage if it is targeted by other commensal bacterial species that have a T6SS apparatus. In this scenario, the *hcp1* mutant would not be able to counterattack T6SS$^+$ commensals. Our results highlight the importance of T6SS-mediated antibacterial activity in host gut colonization. A deeper understanding of pathogen strategies in the battle to colonize the gut could lead to previously unidentified therapeutic strategies.

Materials and Methods

Ethics Statement. Experiments involving animals were performed in accordance with National Institutes of Health (NIH) guidelines, the Animal Welfare Act, and US federal law. All animal experiments were approved by the Stanford University Administrative Panel on Laboratory Animal Care (APLAC) and were overseen by the Institutional Animal Care and Use Committee (IACUC) under Protocol ID 12826. Animals were housed in a centralized research animal facility certified by the Association of Assessment and Accreditation of Laboratory Animal Care (AAALAC) International.

Mouse Strains and Husbandry. The 129x1/SvJ and C57BL/6 mice were obtained from The Jackson Laboratory. Male and female mice (5–8 wk old) were housed under specific pathogen-free conditions in filter-top cages that were changed weekly by veterinary personnel. Sterile water and food were provided ad libitum. Mice were given 1 wk to acclimate to the Stanford Research Animal Facility before experimentation. When specified, an antibiotic mixture [1 g/L ampicillin, 0.5 g/L vancomycin, 1 g/L neomycin, and 1 g/L metronidazole (AVNM)] was added in drinking water for 2 wk to reduce microbiota concentration in the host gut and was then removed 16 h before mice infection.

Mouse Infections. Food and antibiotics in drinking water were removed 16 h before all mouse infections. Mice were infected via oral gavage with 10^8 cfus and 10^9 cfus in 100 μL of PBS for 129x1/SvJ and C57BL/6 mice, respectively. In the coinfection model, mice were inoculated via oral gavage with an equal mixture of strains in 100 μL of PBS. For *S.* Typhimurium and *K. oxytoca* coinfection experiments, mice were first treated with an antibiotic mixture (AVNM) for 2 wk. After 2 wk, mice were switched to regular drinking water and fasted for 16 h. After fasting, mice were inoculated with 10^8 *K. oxytoca* orally. After 8 h of recovery, mice were fasted once again for 16 h before oral inoculation with 10^8 *S.* Typhimurium. *K. oxytoca* was plated on MacConkey plates immediately before inoculation with *S.* Typhimurium to check colonization levels.

Bacterial Strains and Growth Conditions. The *S.* Typhimurium strains used in this study were derived from the streptomycin-resistant parental strain SL1344. The different mutant strains were engineered by replacing the target gene with that of a kanamycin-resistance cassette using the one-step inactivation method (64). Genetic manipulations were originally made in the *S.* Typhimurium LT2 background before being transferred to SL1344 by P22 transduction. All deletions were constructed as described by Maier et al., with P22 phage transduction to insert the deleted genomic region into the WT strain (65) (Table S1). All constructs were verified by PCR. All *S.* Typhimurium strains were grown at 37 °C with aeration in Luria-Bertani (LB) medium containing the appropriate antibiotics: 200 μg/mL streptomycin, 40 μg/mL kanamycin, and 8 μg/mL chloramphenicol. For mouse inoculation, an overnight culture of bacteria was spun down and washed with PBS before resuspension to obtain the desired concentration.

E. coli JB2 commensal strain was kindly provided by M. Raffatellu, University of California, Irvine, CA (28). Commensal bacterial strains used in this study were isolated from WT C57BL/6 and 129x1/SvJ mice housed at Stanford University (Table S1). Fecal pellets were streaked on BHI agar (BD Difco) plates supplemented with 5% (vol/vol) defibrinated sheep's blood (Hemostat Laboratories), followed by aerobic incubation at 37 °C for 24 h. Individual colonies were picked, grown up in Luria broth, and frozen at −80 °C in 10% (vol/vol) glycerol. Individual isolates were characterized by 16S rDNA sequencing. Briefly, colonies were resuspended in 100 μL of PBS and boiled for 10 min at 95 °C. The 16S gene was amplified by PCR by using Phusion High-Fidelity DNA polymerase (Thermo/Fisher) and primers 63F (CAG GCC TAA CAC ATG CAA GTC) and 1387R (GCC CGG GAA CGT ATT CAC CG). PCR products were sequenced using the 63F and 1387R primers and classified using the Michigan State University Ribosomal Database Project classifier function and the National Center for Biotechnology Information (NCBI) BLAST program.

***S.* Typhimurium Burden in Tissues.** After collection of fresh fecal pellets, animals were killed at the specified time points. Animals were euthanized by cervical dislocation. Sterile dissection tools were used to isolate individual organs, which were weighed before homogenization. Visible PPs (three to six per mouse) were isolated from the small intestine using sterile fine-tip straight tweezers and scalpels. PPs, MLNs, spleens, and livers were collected in 1 mL of PBS. The small intestine, cecum, and colon were collected in 3 mL of PBS. Homogenates were then serially diluted and plated onto LB agar containing the appropriate antibiotics to enumerate colony-forming units (cfus) per g of tissue. For coinfections, several dilutions were plated to ensure adequate colonies (>100 cfus per sample) for subsequent patch plating to determine strain abundance.

Bacterial Two-Hybrid Assay. The adenylate cyclase-based bacterial two-hybrid technique (66) was used as previously published (67). Briefly, proteins to be tested were fused to the isolated T18 and T25 catalytic domains of the *Bordetella* adenylate cyclase. Plasmids encoding protein fusion between the Hcp/Tae4 proteins and the T18 or T25 domain were obtained by restriction-free cloning as previously published (68) using pairs ECO2255/ECO2257 (T18-Hcp1), ECO2256/ECO2257 (T18-Hcp2), and ECO2253/ECO2254 (T25-Tae4). After transformation of the two plasmids producing the fusion proteins into the reporter BTH101 strain, plates were incubated at 30 °C for 24 h. Three independent colonies for each transformation were inoculated into 600 μL of LB medium supplemented with ampicillin, kanamycin, and isopropyl β-D-1-thiogalactopyranoside (IPTG, 0.5 mM). After overnight growth at 30 °C, 10 μL of each culture were dropped onto LB plates supplemented with ampicillin, kanamycin, IPTG, and bromo-chloro-indolyl-galactopyrannoside (40 μg/mL) and incubated for 16 h at 30 °C. The experiments were done at least in triplicate, and a representative result is shown.

Hcp1, Hcp2, and Tae4 Protein Purification. Plasmids encoding the Hcp proteins fused to an N-terminal 6×His tag or the Tae4 protein fused to a 6×His-TRX-TEV tag were obtained by restriction-free cloning as previously published (68) using pairs ECO2217/ECO2219 (Hcp1), ECO2218/ECO2219 (Hcp2), and ECO2220/ECO2221 (Tae4). The 6×His-tagged Hcp proteins were purified by ion metal affinity chromatography (IMAC) from 0.5 L of culture of *E. coli* BL21(DE3) cells bearing the pRSF-1 plasmid derivatives grown at 37 °C to an $OD_{600} = 0.6$ and gene induction with 500 μM IPTG for 18 h at 16 °C. Bacteria were harvested, resuspended to an $OD_{600} = 80$ in buffer A (50 mM Tris·HCl, pH 8.0, 150 mM NaCl) supplemented with 1 mM EDTA, 100 μg/mL lysozyme, 100 μg/mL DNase, 10 mM $MgCl_2$, and protease inhibitors (Complete; Roche). Bacteria were broken using an Emulsiflex apparatus, and the insoluble material was discarded by centrifugation for 30 min at 55,000 × *g*. All of the subsequent purification steps were performed using an AKTA FPLC system. First, the soluble fraction was loaded into a 5-mL HisTrap column (GE Health Sciences). After extensive washing with a 0- to 20-mM gradient of imidazole, the Hcp proteins were eluted using 500 mM imidazole in buffer A. The pooled fractions were dialyzed overnight at 4 °C on 3,500-Da pore membrane tubing (Spectra/Por; Spectrumlabs) in buffer A supplemented with 10 mM imidazole. The 6×His-TRX-TEV–tagged Tae4 protein was purified using an identical protocol, except that purified 6×His-tagged tobacco etch virus (TEV) protease and 1.2 mM dithiotreitol were added in the membrane tubing during dialysis. The cleaved, untagged Tae4 protein was obtained in the flow-through of a second IMAC.

Complementation of *tae4* and *hcp1*. To complement *tae4* and *hcp1*, both genes were individually amplified by PCR from *S.* Typhimurium (SL1344) genomic DNA using Phusion DNA polymerase (NEB). After digestion with the appropriate enzymes, the products were ligated to the plasmid pDiGc using T4 ligase (NEB). After heat-shock transformation into competent cells, clones were screened by PCR using primers TSD107 along with either KL1 or KL3, for *tae4* and *hcp1*, respectively. Positive clone inserts were sequenced using TSD107 and then electroporated in *S.* Typhimurium mutant strains. Competition was performed as described, except 0.05% arabinose or 0.1% glucose was added to respectively induce or repress the corresponding cloned gene. Empty pDiGc was used as a negative control.

Hcp/Tae4 Copurification Assay. Two hundred micrograms of the purified Tae4 protein were diluted 10 times in PBS buffer and biotinylated using EZ-Link NHS-PEG4-Biotin (Thermo-Fisher Scientific), mixed with 100 μg of purified 6×His-tagged Hcp1 or Hcp2 protein and 60 μL of Pureproteome Nickel magnetic beads (Millipore). After incubation for 1 h at 4 °C on a wheel, the flow-through was collected and the beads were washed three times with 8 volumes of buffer A and eluted in buffer A supplemented with 0.5 M imidazole. The total, flow-through, first wash, and elution samples were then resuspended in Laemmli buffer and boiled for 10 min, and the proteins were resolved by SDS/PAGE. After transfer onto nitrocellulose, the Hcp and Tae4 proteins were detected using monoclonal anti-5×His antibody (QIAGEN) and streptavidin-coupled to alkaline phosphatase (Molecular Probes, Life Technologies), respectively.

Hcp1 and Hcp2 Structure Modeling. The homology models of Hcp1 were built using *Coot* (69) according to a Multalin alignment with the closest homolog, the enteroaggregative *E. coli* (EAEC) Hcp protein (PDB ID code 4HKH) (70).

In Vitro Competition. Overnight cultures of bacteria were spun down and washed with PBS before resuspension at 10^{10} bacteria per milliliter. Then, 10 μL of each resuspension were spotted on an LB plate supplemented with 0.05% of porcine bile salts (Sigma-Aldrich) and grow at 37 °C for 48 h. Spots were serially diluted and plated on LB supplemented with the appropriate antibiotic, or MacConkey agar (Fisher Scientific). Bait recovered was calculated as the ratio of total bait cfus divided by total *Salmonella* cfus recovered after scraping and counting on selective plates. For in vitro competition in anaerobic conditions, a similar protocol was followed, with the exception that bacteria were grown at 37 °C in an anaerobic chamber for 96 h on blood plates [horse blood from Sigma-Aldrich at 10% in Brain–Heart Infusion (BHI) agar medium].

Monitoring Fecal Shedding of *S.* Typhimurium. Individual mice were identified by distinct tail markings and tracked throughout the duration of infection. Between two and three fresh fecal pellets were collected directly into Eppendorf tubes and weighed at the indicated time points. Pellets were resuspended in 500 mL of PBS, and colony-forming units per gram of feces were determined by plating serial dilutions on LB agar plates with the appropriate antibiotics.

Statistical Analyses. Prism (GraphPad) was used to perform all statistical analyses. Differences in cfus and strain composition between groups were examined by unpaired nonparametric Mann–Whitney *U* tests. Differences for in vitro competition were examined by Student *t* test. Differences in competitive index were examined by Dunnett tests. Significance was defined by $P < 0.05$ (*), $P < 0.01$ (**), $P < 0.001$ (***), and $P < 0.0001$ (****).

ACKNOWLEDGMENTS. We thank the members of the D.M.M. and E.C. groups for fruitful discussion and constant support; Katharine Ng and Justin Sonnenburg for sharing commensal strains; and anonymous reviewers for critical and constructive comments. The *E. coli* JB2 commensal strain was kindly provided by M. Raffatellu. Work in the D.M.M. laboratory is supported by Award AI116059 from National Institute of Allergy and Infectious Diseases and by the Burroughs Wellcome Fund. Work in the E.C. laboratory is supported by the Centre National de la Recherche Scientifique, the Aix-Marseille Université, and Agence Nationale de la Recherche Grant ANR-14-CE14-0006-02.

1. Leatham MP, et al. (2009) Precolonized human commensal Escherichia coli strains serve as a barrier to E. coli O157:H7 growth in the streptomycin-treated mouse intestine. *Infect Immun* 77(7):2876–2886.
2. van der Waaij D, Berghuis-de Vries JM, Lekkerkerk Lekkerkerk-v (1971) Colonization resistance of the digestive tract in conventional and antibiotic-treated mice. *J Hyg (Lond)* 69(3):405–411.
3. Ivanov II, et al. (2009) Induction of intestinal Th17 cells by segmented filamentous bacteria. *Cell* 139(3):485–498.
4. Mazmanian SK, Round JL, Kasper DL (2008) A microbial symbiosis factor prevents intestinal inflammatory disease. *Nature* 453(7195):620–625.
5. Round JL, Mazmanian SK (2009) The gut microbiota shapes intestinal immune responses during health and disease. *Nat Rev Immunol* 9(5):313–323.
6. Hooper LV (2009) Do symbiotic bacteria subvert host immunity? *Nat Rev Microbiol* 7(5):367–374.
7. Hibbing ME, Fuqua C, Parsek MR, Peterson SB (2010) Bacterial competition: Surviving and thriving in the microbial jungle. *Nat Rev Microbiol* 8(1):15–25.
8. Ferreyra JA, Ng KM, Sonnenburg JL (2014) The enteric two-step: Nutritional strategies of bacterial pathogens within the gut. *Cell Microbiol* 16(7):993–1003.
9. Hood RD, et al. (2010) A type VI secretion system of Pseudomonas aeruginosa targets a toxin to bacteria. *Cell Host Microbe* 7(1):25–37.
10. Alcoforado Diniz J, Liu YC, Coulthurst SJ (2015) Molecular weaponry: Diverse effectors delivered by the Type VI secretion system. *Cell Microbiol* 17(12):1742–1751.
11. Cascales E (2008) The type VI secretion toolkit. *EMBO Rep* 9(8):735–741.
12. Bingle LE, Bailey CM, Pallen MJ (2008) Type VI secretion: A beginner's guide. *Curr Opin Microbiol* 11(1):3–8.
13. Jiang F, Waterfield NR, Yang J, Yang G, Jin Q (2014) A Pseudomonas aeruginosa type VI secretion phospholipase D effector targets both prokaryotic and eukaryotic cells. *Cell Host Microbe* 15(5):600–610.
14. MacIntyre DL, Miyata ST, Kitaoka M, Pukatzki S (2010) The Vibrio cholerae type VI secretion system displays antimicrobial properties. *Proc Natl Acad Sci USA* 107(45):19520–19524.
15. Pukatzki S, Ma AT, Revel AT, Sturtevant D, Mekalanos JJ (2007) Type VI secretion system translocates a phage tail spike-like protein into target cells where it cross-links actin. *Proc Natl Acad Sci USA* 104(39):15508–15513.
16. Bleves S, Sana TG, Voulhoux R (2014) The target cell genus does not matter. *Trends Microbiol* 22(6):304–306.
17. Sana TG, et al. (2015) Internalization of Pseudomonas aeruginosa strain PAO1 into epithelial cells is promoted by interaction of a T6SS effector with the microtubule network. *MBio* 6(3):e00712.
18. Sana TG, et al. (2012) The second type VI secretion system of Pseudomonas aeruginosa strain PAO1 is regulated by quorum sensing and Fur and modulates internalization in epithelial cells. *J Biol Chem* 287(32):27095–27105.
19. Zoued A, et al. (2014) Architecture and assembly of the type VI secretion system. *Biochim Biophys Acta* 1843(8):1664–1673.
20. Basler M, Pilhofer M, Henderson GP, Jensen GJ, Mekalanos JJ (2012) Type VI secretion requires a dynamic contractile phage tail-like structure. *Nature* 483(7388):182–186.
21. Durand E, et al. (2015) Biogenesis and structure of a type VI secretion membrane core complex. *Nature* 523(7562):555–560.
22. Leiman PG, et al. (2009) Type VI secretion apparatus and phage tail-associated protein complexes share a common evolutionary origin. *Proc Natl Acad Sci USA* 106(11):4154–4159.
23. Silverman JM, et al. (2013) Haemolysin coregulated protein is an exported receptor and chaperone of type VI secretion substrates. *Mol Cell* 51(5):584–593.
24. Kapitein N, et al. (2013) ClpV recycles VipA/VipB tubules and prevents non-productive tubule formation to ensure efficient type VI protein secretion. *Mol Microbiol* 87(5):1013–1028.
25. Collins FM, Carter PB (1978) Growth of salmonellae in orally infected germfree mice. *Infect Immun* 21(1):41–47.
26. Endt K, et al. (2010) The microbiota mediates pathogen clearance from the gut lumen after non-typhoidal Salmonella diarrhea. *PLoS Pathog* 6(9):e1001097.
27. Thiennimitr P, Winter SE, Bäumler AJ (2012) Salmonella, the host and its microbiota. *Curr Opin Microbiol* 15(1):108–114.

28. Behnsen J, et al. (2014) The cytokine IL-22 promotes pathogen colonization by suppressing related commensal bacteria. *Immunity* 40(2):262–273.
29. Liu JZ, et al. (2012) Zinc sequestration by the neutrophil protein calprotectin enhances Salmonella growth in the inflamed gut. *Cell Host Microbe* 11(3):227–239.
30. Raffatellu M, et al. (2009) Lipocalin-2 resistance confers an advantage to Salmonella enterica serotype Typhimurium for growth and survival in the inflamed intestine. *Cell Host Microbe* 5(5):476–486.
31. Stecher B, et al. (2012) Gut inflammation can boost horizontal gene transfer between pathogenic and commensal Enterobacteriaceae. *Proc Natl Acad Sci USA* 109(4): 1269–1274.
32. Winter SE, et al. (2010) Gut inflammation provides a respiratory electron acceptor for Salmonella. *Nature* 467(7314):426–429.
33. Blondel CJ, Jiménez JC, Contreras I, Santiviago CA (2009) Comparative genomic analysis uncovers 3 novel loci encoding type six secretion systems differentially distributed in Salmonella serotypes. *BMC Genomics* 10:354.
34. Russell AB, et al. (2012) A widespread bacterial type VI secretion effector superfamily identified using a heuristic approach. *Cell Host Microbe* 11(5):538–549.
35. Benz J, Reinstein J, Meinhart A (2013) Structural insights into the effector-immunity system Tae4/Tai4 from Salmonella typhimurium. *PLoS One* 8(6):e67362.
36. Brunet YR, et al. (2015) H-NS silencing of the Salmonella pathogenicity island 6-encoded type VI secretion system limits Salmonella enterica serovar Typhimurium interbacterial killing. *Infect Immun* 83(7):2738–2750.
37. Lam LH, Monack DM (2014) Intraspecies competition for niches in the distal gut dictate transmission during persistent Salmonella infection. *PLoS Pathog* 10(12): e1004527.
38. Miyata ST, Bachmann V, Pukatzki S (2013) Type VI secretion system regulation as a consequence of evolutionary pressure. *J Med Microbiol* 62(Pt 5):663–676.
39. Silverman JM, Brunet YR, Cascales E, Mougous JD (2012) Structure and regulation of the type VI secretion system. *Annu Rev Microbiol* 66:453–472.
40. Sana TG, Soscia C, Tonglet CM, Garvis S, Bleves S (2013) Divergent control of two type VI secretion systems by RpoN in Pseudomonas aeruginosa. *PLoS One* 8(10):e76030.
41. Bachmann V, et al. (2015) Bile salts modulate the mucin-activated type VI secretion system of pandemic Vibrio cholerae. *PLoS Negl Trop Dis* 9(8):e0004031.
42. Durand E, Cambillau C, Cascales E, Journet L (2014) VgrG, Tae, Tle, and beyond: The versatile arsenal of type VI secretion effectors. *Trends Microbiol* 22(9):498–507.
43. Shneider MM, et al. (2013) PAAR-repeat proteins sharpen and diversify the type VI secretion system spike. *Nature* 500(7462):350–353.
44. Unterweger D, et al. (2015) Chimeric adaptor proteins translocate diverse type VI secretion system effectors in Vibrio cholerae. *EMBO J* 34(16):2198–2210.
45. Flaugnatti N, et al. (2016) A phospholipase A1 antibacterial Type VI secretion effector interacts directly with the C-terminal domain of the VgrG spike protein for delivery. *Mol Microbiol* 99(6):1099–1118.
46. Gulati AS, et al. (2012) Mouse background strain profoundly influences Paneth cell function and intestinal microbial composition. *PLoS One* 7(2):e32403.
47. Willing BP, Russell SL, Finlay BB (2011) Shifting the balance: Antibiotic effects on host-microbiota mutualism. *Nat Rev Microbiol* 9(4):233–243.
48. Ma AT, Mekalanos JJ (2010) In vivo actin cross-linking induced by Vibrio cholerae type VI secretion system is associated with intestinal inflammation. *Proc Natl Acad Sci USA* 107(9):4365–4370.
49. Pukatzki S, et al. (2006) Identification of a conserved bacterial protein secretion system in Vibrio cholerae using the Dictyostelium host model system. *Proc Natl Acad Sci USA* 103(5):1528–1533.
50. Basler M, Ho BT, Mekalanos JJ (2013) Tit-for-tat: Type VI secretion system counterattack during bacterial cell-cell interactions. *Cell* 152(4):884–894.
51. Brunet YR, Espinosa L, Harchouni S, Mignot T, Cascales E (2013) Imaging type VI secretion-mediated bacterial killing. *Cell Reports* 3(1):36–41.
52. Brunet YR, Hénin J, Celia H, Cascales E (2014) Type VI secretion and bacteriophage tail tubes share a common assembly pathway. *EMBO Rep* 15(3):315–321.
53. Mougous JD, et al. (2006) A virulence locus of Pseudomonas aeruginosa encodes a protein secretion apparatus. *Science* 312(5779):1526–1530.
54. Zhou Y, et al. (2012) Hcp family proteins secreted via the type VI secretion system coordinately regulate Escherichia coli K1 interaction with human brain microvascular endothelial cells. *Infect Immun* 80(3):1243–1251.
55. Gopinath S, Lichtman JS, Bouley DM, Elias JE, Monack DM (2014) Role of disease-associated tolerance in infectious superspreaders. *Proc Natl Acad Sci USA* 111(44): 15780–15785.
56. Faber F, et al. (2016) Host-mediated sugar oxidation promotes post-antibiotic pathogen expansion. *Nature* 534(7609):697–699.
57. Zhang H, et al. (2013) Structure of the type VI effector-immunity complex (Tae4-Tai4) provides novel insights into the inhibition mechanism of the effector by its immunity protein. *J Biol Chem* 288(8):5928–5939.
58. Chow J, Mazmanian SK (2010) A pathobiont of the microbiota balances host colonization and intestinal inflammation. *Cell Host Microbe* 7(4):265–276.
59. Lertpiriyapong K, et al. (2012) Campylobacter jejuni type VI secretion system: Roles in adaptation to deoxycholic acid, host cell adherence, invasion, and in vivo colonization. *PLoS One* 7(8):e42842.
60. Fu Y, Waldor MK, Mekalanos JJ (2013) Tn-Seq analysis of Vibrio cholerae intestinal colonization reveals a role for T6SS-mediated antibacterial activity in the host. *Cell Host Microbe* 14(6):652–663.
61. Russell AB, et al. (2014) A type VI secretion-related pathway in Bacteroidetes mediates interbacterial antagonism. *Cell Host Microbe* 16(2):227–236.
62. Coyne MJ, Roelofs KG, Comstock LE (2016) Type VI secretion systems of human gut Bacteroidales segregate into three genetic architectures, two of which are contained on mobile genetic elements. *BMC Genomics* 17(1):58.
63. Chatzidaki-Livanis M, Geva-Zatorsky N, Comstock LE (2016) Bacteroides fragilis type VI secretion systems use novel effector and immunity proteins to antagonize human gut Bacteroidales species. *Proc Natl Acad Sci USA* 113(13):3627–3632.
64. Datsenko KA, Wanner BL (2000) One-step inactivation of chromosomal genes in Escherichia coli K-12 using PCR products. *Proc Natl Acad Sci USA* 97(12):6640–6645.
65. Maier L, et al. (2013) Microbiota-derived hydrogen fuels Salmonella typhimurium invasion of the gut ecosystem. *Cell Host Microbe* 14(6):641–651.
66. Karimova G, Pidoux J, Ullmann A, Ladant D (1998) A bacterial two-hybrid system based on a reconstituted signal transduction pathway. *Proc Natl Acad Sci USA* 95(10): 5752–5756.
67. Battesti A, Bouveret E (2012) The bacterial two-hybrid system based on adenylate cyclase reconstitution in Escherichia coli. *Methods* 58(4):325–334.
68. Aschtgen MS, Bernard CS, De Bentzmann S, Lloubès R, Cascales E (2008) SciN is an outer membrane lipoprotein required for type VI secretion in enteroaggregative Escherichia coli. *J Bacteriol* 190(22):7523–7531.
69. Emsley P, Lohkamp B, Scott WG, Cowtan K (2010) Features and development of Coot. *Acta Crystallogr D Biol Crystallogr* 66(Pt 4):486–501.
70. Douzi B, et al. (2014) Crystal structure and self-interaction of the type VI secretion tail-tube protein from enteroaggregative Escherichia coli. *PLoS One* 9(2):e86918.
71. Gully D, Bouveret E (2006) A protein network for phospholipid synthesis uncovered by a variant of the tandem affinity purification method in *Escherichia coli*. *Proteomics* 6(1):282–293.
72. Helaine S, et al. (2010) Dynamics of intracellular bacterial replication at the single cell level. *Proc Natl Acad Sci USA* 107(8):3746–3751.
73. Marchesi JR, et al. (1998) Design and evaluation of useful bacterium-specific PCR primers that amplify genes coding for bacterial 16S rRNA. *Appl Environ Microbiol* 64(2):795–799.

Supporting Information

Sana et al. 10.1073/pnas.1608858113

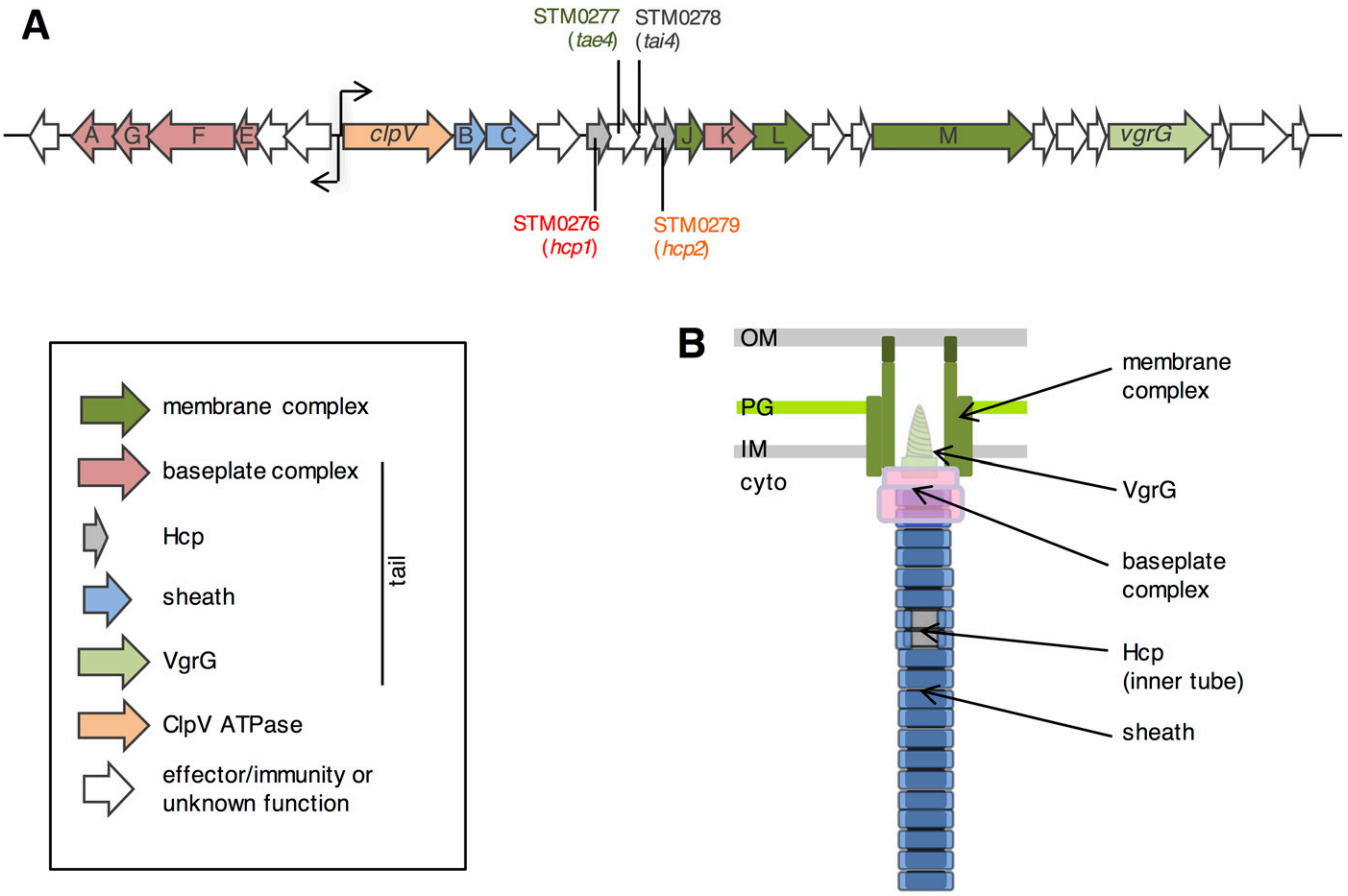

Fig. S1. Representation of the SPI-6 type VI secretion system. (*A*) Representation of the SPI-6 genetic locus starting at STM0266 and ending at STM0292. (*B*) Schematic representation of a prototypical T6SS apparatus. Genes encoding the sheath components (TssB/TssC), the ClpV ATPase, the VgrG spike protein, the membrane and baseplate complexes, and the Hcp proteins are colored in light blue, orange, light green, dark green, pink, and gray, respectively, as indicated and within the T6SS architecture scheme. *hcp1*, *hcp2*, and *tae4* are highlighted, respectively, in red, orange and green, a color code that is conserved all along the figures of this manuscript. cyto, cytoplasm; IM, inner membrane; OM, outer membrane; PG, peptidoglycan layer.

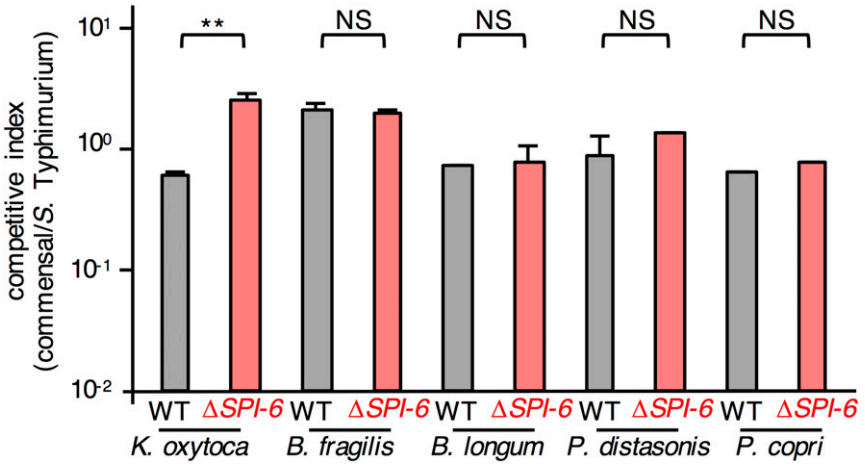

Fig. S2. *Salmonella* does not compete in a T6SS-dependent manner with *Bacteroides fragilis, Bifidobacterium longum, Parabacteroides distasonis,* and *Prevotella copri* when grown anaerobically on blood plates, a condition in which the SPI-6 T6SS is active, as shown by *S.* Typhimurium's killing of *K. oxytoca*. WT and mutant *S.* Typhimurium strains were incubated with commensal strains to assess T6SS-dependent killing. The indicated *S.* Typhimurium attacker strain was mixed with respective commensal bacteria prey at a 1:1 ratio and incubated for 96 h on a blood agar plate placed in an anaerobic chamber at 37 °C. Recovered mixtures were plated onto selective media. Statistical significance is shown based a Student's *t* test corresponding to the values of the WT strain (NS, not significant; $^{**}P < 0.01$).

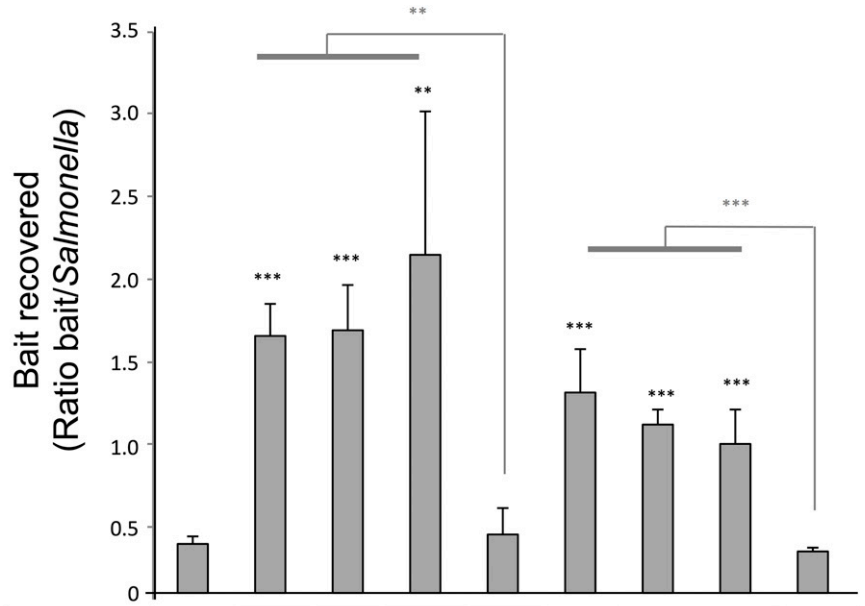

Strain	WT	Δ*hcp1*	Δ*hcp1*	Δ*hcp1*	Δ*hcp1*	Δ*tae4*	Δ*tae4*	Δ*tae4*	Δ*tae4*
Plasmid	pDiGc	pDiGc	pDiGc	pDiGc-*hcp1*	pDiGc-*hcp1*	pDiGc	pDiGc	pDiGc-*tae4*	pDiGc-*tae4*
Glucose	-	+	-	+	-	+	-	+	-
Arabinose	-	-	+	-	+	-	+	-	+

Fig. S3. Complementation of *hcp1* and *tae4* mutations. WT and mutant *S.* Typhimurium strains were incubated with *Klebsiella oxytoca* at a 1:1 ratio and incubated for 48 h on LB supplemented with 0.05% bile salts at 37 °C, to assess T6SS-dependent killing. Recovered mixtures were plated onto selective media. pDiGc is the control empty plasmid, and *hcp1* and *tae4* are encoded under the arabinose-inducible promoter, which is repressed by glucose. Glucose and arabinose were added at a final concentration of 0.5% and 0.05%, respectively, where indicated. Statistical significance is shown based on Student's *t* test corresponding to the values of the WT strain ($^{**}P < 0.01$; $^{***}P < 0.001$).

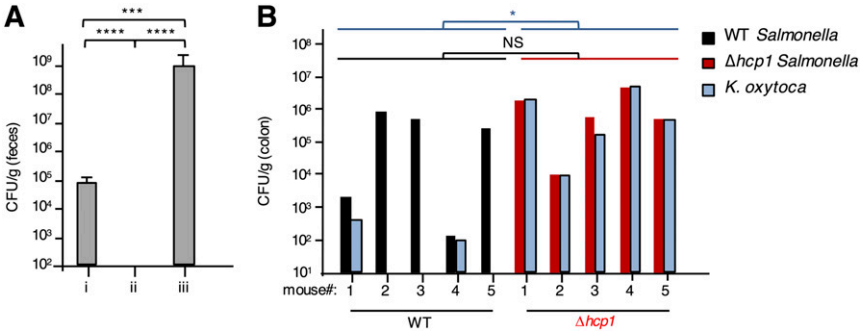

Fig. S4. SPI-6 antibacterial activity is active in colons. (*A*) The 129x1/SvJ mice feces were plated on MacConkey agar pre-antibiotics treatment (bar i), post-antibiotics treatment (bar ii), or postcolonization with *K. oxytoca* (bar iii). (*B*) The 129x1/SvJ mice were treated with antibiotics for 2 wk before colonization with *K. oxytoca*. The day after, mice were infected orally with 10^8 WT or Δ*hcp1* mutant *S.* Typhimurium cells. Colons were harvested and plated at day 3 postinfection. Statistical significance is shown based on Mann–Whitney *U* test (NS, not significant; **P* < 0.05; ****P* < 0.001; *****P* < 0.0001).

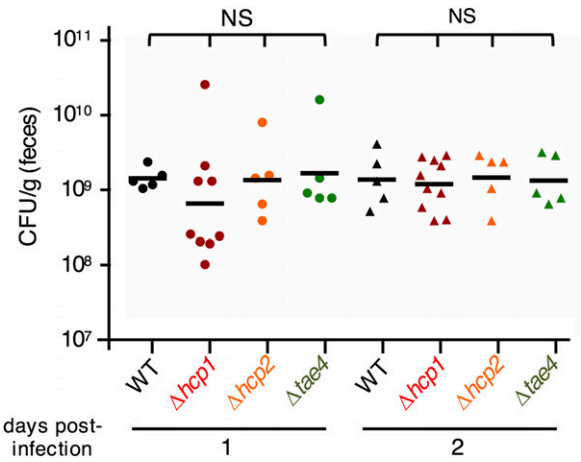

Fig. S5. SPI-6 antibacterial activity is not necessary to establish in the host gut of mice treated with antibiotics. The 129x1/SvJ mice were orally treated with a mixture of antibiotics for 2 wk and then orally infected with 10^8 cells of the indicated *S.* Typhimurium strain. Feces were collected at day 1 and 2 and plated over time on *Salmonella* selective medium. Every data point represents one mouse, and the line represents the geometric mean. Statistical significance is shown based on Mann–Whitney *U* test (NS, not significant).

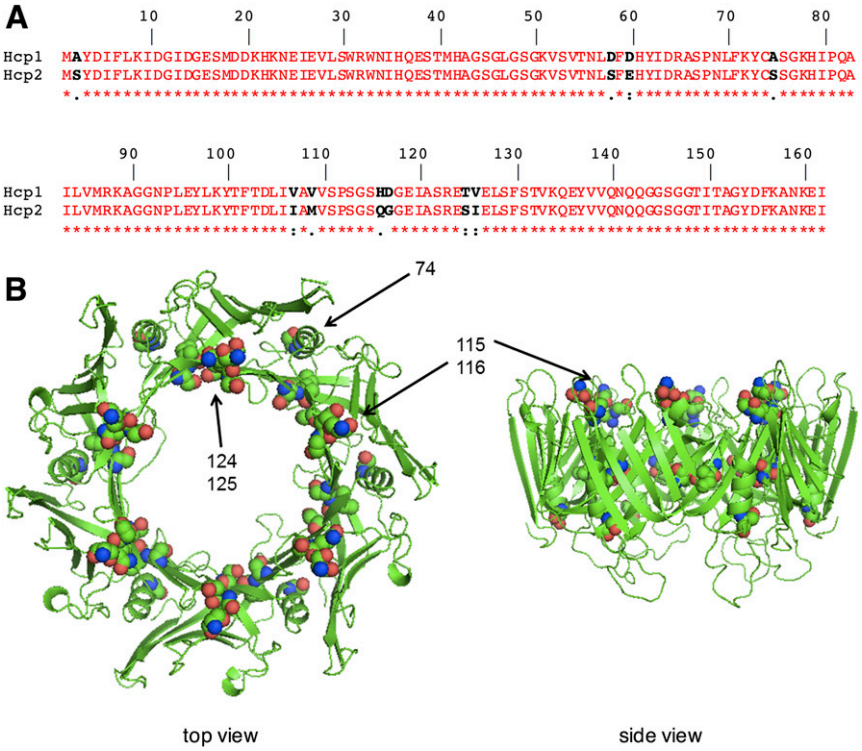

Fig. S6. Comparison of the Hcp1 and Hcp2 sequences and structures. (*A*) Sequence alignment of Hcp1 and Hcp2. Identical and different residues are indicated in red and black, respectively. (*B*) Molecular modeling of the Hcp1 hexameric structures. All conserved residues are shown in ribbon whereas the residues that differ between *Hcp1* and *Hcp2* are shown in balls. Two of the four variant residues face the lumen (positions 124 and 125) whereas two (positions 115 and 116) are located at the hexamer–hexamer interface within the tube.

Table S1. Strains, plasmids, and oligonucleotides used in this study

Strains/plasmids/ oligonucleotides	Description/sequence*	Source
Commensal strains		
Klebsiella oxytoca TS1	Isolated from 129x1/SvJ mice feces	This work
Klebsiella variicola KL11	Isolated from C57BL/6 mice feces	This work
Escherichia coli JB2	Isolated from C57BL/6 mice feces	(28)
Enterobacter cloacae KL1	Isolated from C57BL/6 mice feces	This work
Bacteroides fragilis NCTC9343	Originally from the American Type Culture Collection (ATCC) bacterial strain collection	J. Sonnenburg
Bifidobacterium longum NCC2705	Originally from the ATCC bacterial strain collection	J. Sonnenburg
Parabacteroides distasonis ATCC 8503	Originally from in the ATCC bacterial strain collection	J. Sonnenburg
Prevotella copri 18205	Originally from the Japan Collection of Microorganisms (JCM) bacterial strain collection	J. Sonnenburg
S. Typhimurium strains		
LT2	LT2 WT	Laboratory collection
SL1344	SL1344 WT	Laboratory collection
SL1344 Δ*SPI-6*	SL1344 *SPI-6*::Km^R	This work
SL1344 Δ*clpV*	SL1344 *clpV*::Km^R	This work
SL1344 Δ*hcp1*	SL1344 *hcp1*::Km^R	This work
SL1344 Δ*hcp2*	SL1344 *hcp2*::Km^R	This work
SL1344 Δ*tae4*	SL1344 *tae4*::Km^R	This work
E. coli strains		
DH5α	F-, *ΔargF-lac phoA supE44 ΔlacZ relA endA thi hsdR*	New England Biolabs
BTH101	F-, *cya araD galE galK rpsL hsdR mcrA mcrB*	(66)
BL21(DE3)	*fhuA lon ompT gal* (*λ DE3*) *dcm ΔhsdS*	New England Biolabs
Plasmids		
pUT18	BACTH plasmid, ColE1, Amp^R, T18 domain of *Bordetella pertussis* Cya	(66)
pT18-Pal	*E. coli pal* gene cloned into pUT18	(71)
pT18-Hcp1	*S.* Typhimurium STM0276 (*hcp1*) gene cloned into pUT18	This work
pT18-Hcp2	*S.* Typhimurium STM0279 (*hcp2*) gene cloned into pUT18	This work
pKT25	BACTH plasmid, pACYC, Kan^R, T25 domain of *B. pertussis* Cya	(66)
pKT25-TolB	*E. coli tolB* gene cloned into pKT25	(71)
pKNT25	BACTH plasmid, pACYC, Kan^R, T25 domain of *B. pertussis* Cya	(66)
pKNT25-Tae4	*S.* Typhimurium STM0277 (*tae4*) gene cloned into pKNT25	This work
pRSF-1	Expression vector, RSF1030, Kan^R, T7 promoter, N-terminal 6×His	Addgene
pRSF-Hcp1	*S.* Typhimurium STM0276 (*hcp1*) gene cloned into pRSF-1	This work
pRSF-Hcp2	*S.* Typhimurium STM0279 (*hcp2*) gene cloned into pRSF-1	This work
pETG20A	Expression vector, Amp^R, T7 promoter, N-terminal TRX-6×His-TEV	Laboratory collection
pETG20A-Tae4	*S.* Typhimurium STM0277 (*tae4*) gene cloned into pETG20A	This work
pDiGc	Inducible expression of dsRed and constitutive expression of GFP	(72)
pDiGc-*hcp1*	Inducible expression of SL1344 *hcp1* and constitutive expression of GFP	This work
pDiGc-*tae4*	Inducible expression of SL1344 *tae4* and constitutive expression of GFP	This work
Oligonucleotides		
TSD5	5′-TATTTTTATGAATTTTTATGTCACAAGGCATAACACATGGTGTAGGCTGGAGCTGCTTC	
TSD6	5′-GCACTACGGACACTTCGAACGGCCGGTTTCAGCAAACGATCATATGAATATCCTCCTTAG	This work
TSD7	5′-GTCCCTGATCTGTATCATTG	This work
TSD8	5′-AGTCAACTGGTTGCCGCAAG	This work
TSD13	5′-AGGTTTATTTTAAGTAAAACTTAATAAGGATATAAAAATGGTGTAGGCTGGAGCTGCTTC	This work
TSD14	5′-CAGACATAACATCTGGCCGGAAAAACAGCCGTTAAATTTCCATATGAATATCCTCCTTAG	This work
TSD15	5′-AGTCCTCTGTTCTCCTGAAG	This work
TSD16	5′-GCATAGCTACCGCACATAAC	This work
TSD17	5′-TCAGGGCTTAATTTAGGTAGTTAAAAGGATAGTAGATATGGTGTAGGCTGGAGCTGCTTC	This work
TSD18	5′-CCAGATATAAATCTGGCCGGAAAAACAGCCGTTAAATTTCCATATGAATATCCTCCTTAG	This work
TSD19	5′-TACGTTCTCTTGCTCTGATG	This work
TSD20	5′-CATAGCTACCGCACATAACC	This work
TSD33	5′-TTTTTATACATCCTGTGAAGTAAAAAAAACCGTAGTGTAGGCTGGAGCTGCTTC	This work
TSD34	5′-ATGGCACATTAATTTGAAGCAGCTCTCATCCGGTCATATGAATATCCTCCTTAG	This work
TSD35	5′-CCGAAGTGTATCTGGCGATGA	This work
TSD83	5′-TTAATGACCTACACAGAATTTTTAGAGGTTAAGCAAAATGGTGTAGGCTGGAGCTGCTTC	This work
TSD84	5′-TATTAACCATTTCACGGCAGTATCCACAGTGTCCCAACTTCATATGAATATCCTCCTTAG	This work
TSD85	5′-GTCCATGAAGATACGTGTTG	This work
TSD86	5′-CATTCCACTTATGCTGAAAG	This work
TS107	5′-TCGGTGCGCTCGTACTGCTC	This work

Table S1. Cont.

Strains/plasmids/ oligonucleotides	Description/sequence*	Source
KL1	5′-AAAAAGACGTCAGGAGGTAATTATGGCTTATGACATTTTTTTG	This work
KL2	5′-TTTTTACCAGGTTTAAATTTCTTTGTTGGCCTT	This work
KL3	5′-AAAAAGACGTCAGGAGGTAATTATGAACAGACCTTCATTCAAT	This work
KL4	5′-TTTTTCACGATGGTGTCACGGCAGTATCCACAGTG	This work
63F	5′-CAGGCCTAACACATGCAAGTC	(73)
1387R	5′-CGGAACATGTGWGGCGGG	(73)
ECO-2255	5′-CGCCACTGCAGGGATTATAAAGATGACGATGACAAGGCTTATGACATTTTTTTGAAAATTGACG-GCATTGAT	This work
ECO-2256	5′-CGCCACTGCAGGGATTATAAAGATGACGATGACAAGTCTTATGACATTTTTCTGAAAATTGACG-GCATTGAC	This work
ECO-2257	5′-CGAGGTCGACGGTATCGATAAGCTTGATATCGAATTCTAGTTAAATTTCTTTGTTGGCCTTGAA-GTCGTAG	This work
ECO-2253	5′-CGGATAACAATTTCACACAGGAAACAGCTATGACCATGAACAGACCTTCATTCAATGAAGCGTGG	This work
ECO-2254	5′-GTTTGCGTAACCAGCCTGATGCGATTGCTGCGGCAGTATCCACAGTGTCCCAAC	This work
ECO-2217	5′-CATCATCACCACAGCCAGGATCCGGCTTATGACATTTTTTTGAAAATTGACGGCATTGAT	This work
ECO-2218	5′-CATCATCACCACAGCCAGGATCCGTCTTATGACATTTTTCTGAAAATTGACGGCATTGAC	This work
ECO-2219	5′-GGCGCGCCGAGCTCGAATTTTAAATTTCTTTGTTGGCCTTGAAGTCGTAG	This work
ECO-2220	5′-GCAGGCTTAGAAAACCTGTACTTCCAGGGTAACAGACCTTCATTCAATGAAGCGTGG	This work
ECO-2221	5′-GCTTTGATCTCGCCTGCCACCGGTACTCACGGCAGTATCCACAGTGTCCCAAC	This work

*Sequence annealing on the target plasmid underlined.